Original Article

RNA sequencing analysis reveals apoptosis induction by hydrogen treatment in endometrial cancer via TNF and NF-κB pathways

Ye Yang[1], Yin-Ping Liu[2], Wei Bao[1], Jun-Song Chen[3], Xiao-Wei Xi[1]

[1]Department of Obstetrics and Gynecology, Shanghai General Hospital, Shanghai Jiao Tong University School of Medicine, Shanghai 200080, China; [2]Department of Obstetrics and Gynecology, Shanghai General Hospital of Nanjing Medical University, Shanghai 200080, China; [3]Department of Systems Biomedicine, Shanghai Jiao Tong University, Shanghai 200241, China

Contributions: (I) Conception and design: Y Yang, XW Xi; (II) Administrative support: XW Xi; (III) Provision of study materials or patients: Y Yang; (IV) Collection and assembly of data: Y Yang, W Bao; (V) Data analysis and interpretation: Y Yang, YP Liu, JS Chen; (VI) Manuscript writing: All authors; (VII) Final approval of manuscript: All authors.

Correspondence to: Xiao-Wei Xi. Shanghai General Hospital, Shanghai Jiao Tong University School of Medicine, 85 Wujin Road, Hongkou, Shanghai 200080, China. Email: xi_xiao_wei1966@163.com.

Background: To evaluate the activity of hydrogen in endometrial cancer and elucidate its underlying molecular mechanisms.

Methods: Ishikawa, HEC1A and AN3CA cells were incubated in DMEM medium with or without hydrogen. RNA sequencing was used to explore the association of hydrogen treatment with signaling pathways and functional genes in endometrial cancer cells. The apoptotic rates of the three endometrial cancer cells were evaluated by fluorescein isothiocyanate (FITC) Annexin V and Annexin V-allophycocyanin (APC)/propidium iodide double staining.

Results: RNA sequencing analysis revealed that hydrogen induced TNF/NF-κB and apoptosis pathways in endometrial cancer cells. The gene sets between hydrogen treatment groups and non-treated groups were mapped in accordance with Kyoto Encyclopedia of Genes and Genomes (KEGG) pathway and Gene Ontology (GO) terms. Hydrogen treatment significantly increased the apoptotic rates of endometrial cancer cells.

Conclusions: Taken together, our data indicate that hydrogen can serve as a therapeutic target for endometrial cancer via TNF/NF-κB pathway and apoptosis induction.

Keywords: Hydrogen; endometrial cancer; TNF-α; NF-κB; apoptosis

Submitted Aug 24, 2019. Accepted for publication Feb 06, 2020.
doi: 10.21037/tcr.2020.03.71
View this article at: http://dx.doi.org/10.21037/tcr.2020.03.71

Introduction

Endometrial cancer is the most common gynecologic malignancy in the United States. Approximately 61,880 new cases of endometrial cancer are estimated in 2019, and 12,160 female patients are expected to die from this disease, according to the American Cancer Society (1). Obesity and diabetes are associated with an increased risk of endometrial cancer, which characterized by the production of tumor necrosis factor-α (TNF-α), interleukin-1β (IL-1β) and IL-6 (2), and these in turn generate oxidative stress via chronic low-level systemic inflammation (3), leading to nuclear factor-κB (NF-κB) activation. Besides, TNF-α and IL-1β, activators of NF-κB, are transcription factors that can regulate apoptosis in endometrial cancer cells (4,5). Hence, this inflammation-cancer interaction introduces issues regarding the roles of inflammatory milieu balance in endometrial cancer, as a double-edged sword that either facilitates tumorigenesis, or enters a feedback cycle of inflammatory cell death. Therefore, we hypothesize that inflammatory micro-environment should be an important metabolism for predicting the risk of endometrial cancer.

In recent years, molecular hydrogen (H_2) has become a promising candidate for type 2 diabetes (6) and metabolic syndrome (7) as well as inflammatory diseases (8). Hydrogen

is safe at a concentration of less than 4.7% in the air. Due to its size-distribution characteristics, H_2 is quite permeable to penetrate bio-membranes and diffuse into the cytosol, mitochondria and nucleus (9). On the contrary, most hydrophilic antioxidants are not able to penetrate across bio-membranes and thus retain on the membranes. Hydrogen can be used as an inert gas at normal body temperature or being dissolved in water or saline up to 1.6 ppm under atmospheric pressure to produce hydrogen water or hydrogen-rich saline. Both hydrogen gas and hydrogen-rich saline are increasingly accepted as anti-inflammatory targets for the treatment of pathological conditions via regulation of cytokine TNF-α, NF-κB and IL-1β expression (10). Additionally, it can attenuate brain (11), hepatic (12), myocardial (13), lung (14) and intestinal ischemia-reperfusion injuries (15) in clinical practice, as well as participate in different types of cell death. The latter observation suggests that if hydrogen can induce the apoptosis of endometrial cancer cells, inflammation-dependent cell death may be proposed as the mechanisms underlying its positive effect in the endometrium, especially proinflammatory cytokines TNF-α, NF-κB and IL-1β. Therefore, this study aimed to investigate the effects of hydrogen on endometrial cancer and elucidate the mechanistic details underpinning hydrogen-induced apoptotic signaling in cancer cells via RNA sequencing. Specifically, annotations based on Kyoto Encyclopedia of Genes and Genomes (KEGG) and Gene Ontology (GO) databases were performed to identify genes and pathways involved in hydrogen-treated endometrial cancer cells.

Methods

Cell culture

Human endometrial cancer cell lines (Ishikawa and HEC1A) were conserved in our laboratory, while AN3CA cells were purchased from FuHeng Cell Center, Shanghai, China. These cells were cultured in Medium DMEM: F12 (1:1, Gibco, USA) containing 10% fetal bovine serum (FBS; Gibco, Gaithersburg, MD, USA), 100 U/mL penicillin G and 100 μg/mL streptomycin (Life Technologies, Inc., Rockville, MD, USA), and maintained in a humidified atmosphere of 5% CO_2 at 37 ℃.

Hydrogen treatment

Hydrogen gas (H_2) was dissolved into water for 6 h under a high pressure of 0.4 MPa until the supersaturation level, by using a hydrogen water producing apparatus (Shanghai Yiquan Investment Limited Partnership Company, Shanghai, China). The hydrogen water was stored in an aluminum bag under atmospheric pressure at 4 ℃ with more than 0.6 mmol/L concentration of H_2. The hydrogen DMEM culture medium (CM) was prepared by mixing 28 mL of sterile hydrogen water (0.7 ppm hydrogen molecule) with 8 mL of 5× DMEM containing 500 U/mL penicillin G and 500 μg/mL streptomycin, 4 mL FBS. The medium was freshly prepared every time.

RNA sequencing

Ishikawa, HEC1A and AN3CA endometrial cancer cells were cultured in hydrogen medium for 24 h. Total RNA was isolated using RNeasy Mini kit (Qiagen, Germany). Paired-end libraries were synthesized with TruSeq™ RNA Sample Preparation Kit (Illumina, USA) according to the TruSeq™ RNA Sample Preparation Guide. Briefly, the poly-A containing mRNA molecules were purified using poly-T oligo-attached magnetic beads. After purification, the obtained mRNA was fragmented into small pieces using divalent cations at 94 ℃ for 8 min. The cleaved RNA fragments were then copied into first strand cDNA using reverse transcriptase and random primers. Afterwards, second strand cDNA synthesis was performed using DNA Polymerase I and RNase H. The resultant cDNA fragments were subjected to an end repair process with the addition of a single "A" base, followed by ligation to adapter sequences. The products were then purified and enriched with PCR, in order to construct the final cDNA library. To verify the insert size and determine the molar concentration, the purified libraries were quantified by Qubit® 2.0 Fluorometer (Life Technologies, USA), and validated using Agilent 2100 bioanalyzer (Agilent Technologies, USA). Cluster was generated by cBot with the library diluted to 10 pM, and then subjected to sequencing using the NovaSeq 6000 System (Illumina, USA). Library construction and sequencing were carried out at Shanghai Sinomics Corporation.

Apoptosis assay

Cell apoptosis was determined using a commercial fluorescein isothiocyanate (FITC) Annexin V Apoptosis Detection kit (BD Pharmingen, San Diego, CA, USA) with Annexin V-allophycocyanin (APC)/propidium iodide (PI) double staining, according to the manufacturer's

instructions. Briefly, cells were collected, washed twice with cold PBS, and resuspended in 1× Binding Buffer (10 mM HEPES, pH 7.4; 140 mM NaCl; 2.5 mM $CaCl_2$, Beyotime, Shanghai, China) at a concentration of 1×10^6 cells/mL. Then, FITC Annexin V (5 μL) and PI (5 μL) were added into the buffer solution (100 μL), followed by incubation at room temperature for 15 min in the dark. The stained cells were analyzed by flow cytometry (FACS Calibur™, BD Biosciences, CA, USA).

Western blot analysis

Total protein was extracted from the treated cells using RIPA buffer. Equal amounts of cellular protein extracts were separated on SDS-polyacrylamide mini-gels, and transferred onto PVDF membranes (Millipore, Billerica, MA, USA) at 300 mA for 1.5 h. The membranes were blocked with 5% BSA (Roche, Mannheim, Germany) for 1 h, and then incubated overnight with the indicated primary antibodies at 4 ℃: antibodies against GAPDH (5174; 1:1,000, CST, USA), NF-κB (8242; 1:1,000, CST, USA), p-NFKBIA (5209; 1:1,000, CST, USA), NFKBIA (4814; 1:1,000, CST, USA), caspase-1 (2225; 1:1,000, CST, USA), caspase-3 (9662; 1:1,000, CST, USA), caspase-9 (ab184786; 1:1,000, Abcam, USA). After washing with Tris-buffered saline with Tween-20 (TBST) (9997, CST, USA) for three times, the membranes were incubated with the corresponding secondary antibodies for 1 h at room temperature. The specific bands of target proteins were visualized by enhanced chemiluminescence (ECL) substrates (Millipore, USA), and quantified using ImageJ software (National Institutes of Health, Bethesda, MD, USA).

Statistical analysis

All statistical analyses were performed using SPSS 22.0 software (IBM Corp, Armonk, NY, USA). Differences between groups were analyzed by Student's *t*-test and one-way ANOVA with Tukey post-test and Fisher's exact test at 95% confidence. Data were expressed as mean ± standard error of the mean (SEM). P value of less than 0.05 was considered statistically significant.

Results

Quality control and mapping of RNA sequencing in hydrogen-treated endometrial cancer cells

RNA sequencing is a common next-generation sequencing technique for assaying genome-wide gene expression profiles. In this study, it was used to explore the roles of signaling pathways and functional gene groups in hydrogen-treated endometrial cancer cells. The quality assessment of sampling results was carried out. The intensity distributions of 6 samples and the differences between hydrogen CM (H-CM) and CM groups for Ishikawa, HEC1A and AN3CA endometrial cancer cells were examined by ring diagram. The reads were aligned to the specific sequences of each sample, as presented in a circular graph via Circos Software package (*Figure 1A*). The mapping relationship among the sequences was existed in this study, with an increased number of genes in the genome, as revealed by sequencing saturation analysis (*Figure 1B*). The greater the depth of sequencing, the higher the number of genes entered a saturation phase. Mapping of regional distribution categorized all the aligned reads into different regions of a gene based on their regulatory elements (*Figure 1C*). Scatterplot graph showed that all genes were plotted on the horizontal and vertical coordinates according to their expression values (*Figure 1D*). Mean expression levels were indicated by fragments per kilobase of exon model per million mapped (FPKM) across samples, and the levels of differential gene expression among 6 samples were calculated by log2 obtained from FPKM values called Log2 (FPKM).

GO and KEGG pathway enrichment analysis of different expressed genes in hydrogen-treated endometrial cancer cells

The characteristics that contributed significantly to different biological functions and signaling pathways were identified from GO and KEGG database between H-CM and CM groups for Ishikawa, HEC1A and AN3CA endometrial cancer cells. GO enrichment analysis (*Figure 2*) revealed that the up-regulated genes in H-CM group were highly correlated to biological process (biological regulation, cellular process, metabolic process and regulation of biological process), cellular component (cell, cell part and organelle) and molecular function (binding). The classification of genes in hydrogen-treated Ishikawa, HEC1A and AN3CA cells were determined by KEGG analysis based on their functions and signaling pathways. As shown in *Figure 3*, most up-regulated genes in H-CM group were classified into metabolism (global and overview maps), genetic information processing (folding, sorting and degradation) and environmental information processing (signal transduction).

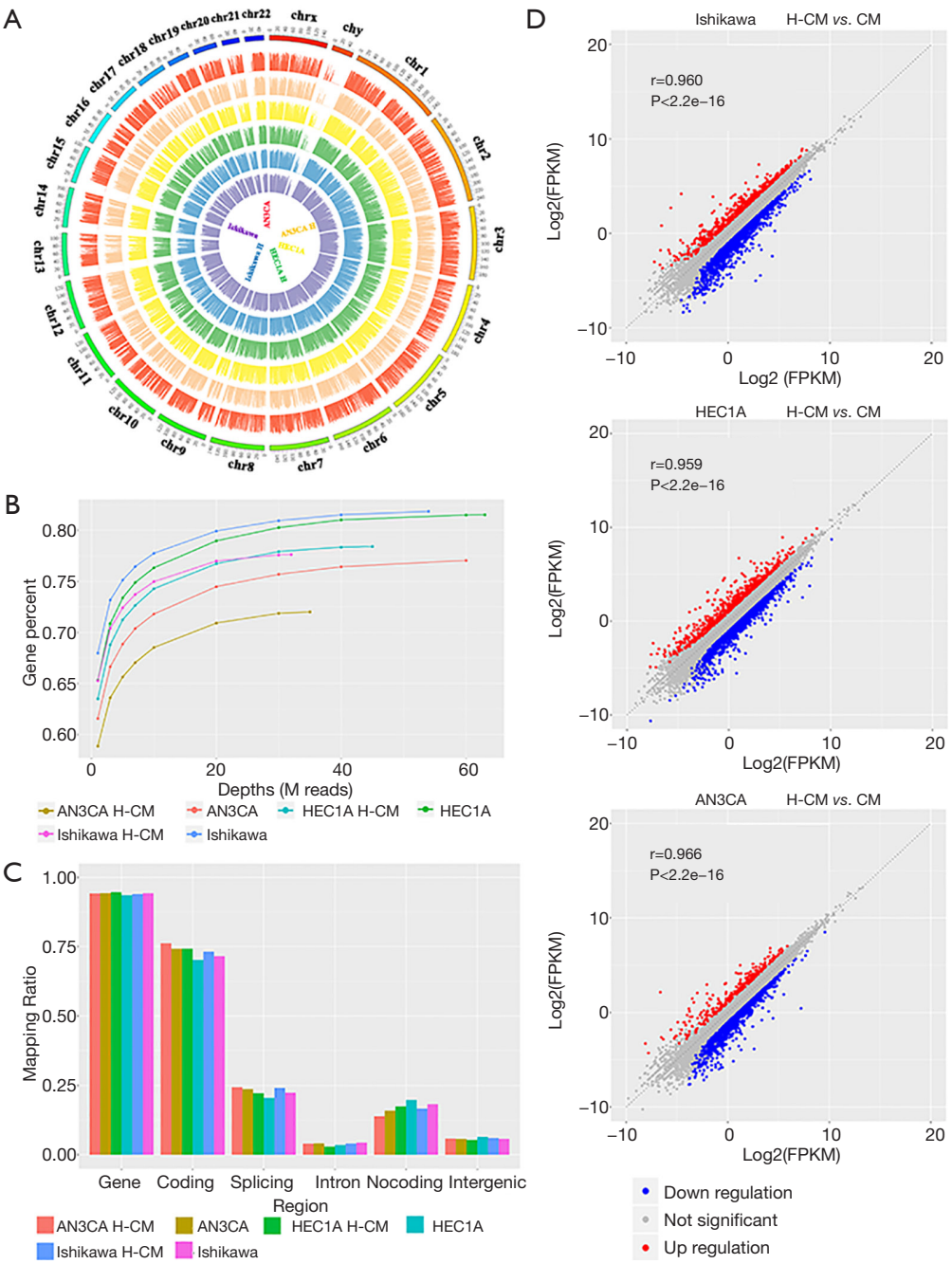

Figure 1 Quality control in hydrogen-treated Ishikawa, HEC1A and AN3CA group (H-CM) compared to control group (CM). (A) Ring diagram, the outermost circle shows the chromosome distribution, and each color inside represents the coverage distribution a sample on the chromosome. (B) Sequence saturation analysis, the abscissa denotes the depth of sequencing, and the ordinate represents the gene percent which is the ratio of the total genes mapped by the sequences to all genes in a genome. (C) Variant discovery reads called mapping ratio under the region distributions of gene, coding, splicing, intron, noncoding and intergenic. The six callers are represented by different colors. The greater the depth of sequencing, the higher the number of genes entered a saturation phase. (D) Scatterplot graph showing the expression level of each gene on the horizontal and vertical coordinates according to the different expression values between groups/samples. Differentially expressed genes among 6 samples were identified through fold-change filtering by Log2(FPKM). The red dots indicate the significant upregulated genes, while the blue dots indicate the significant downregulated genes. The gray dots indicate not significant regulated genes. H-CM, hydrogen culture medium; CM, culture medium.

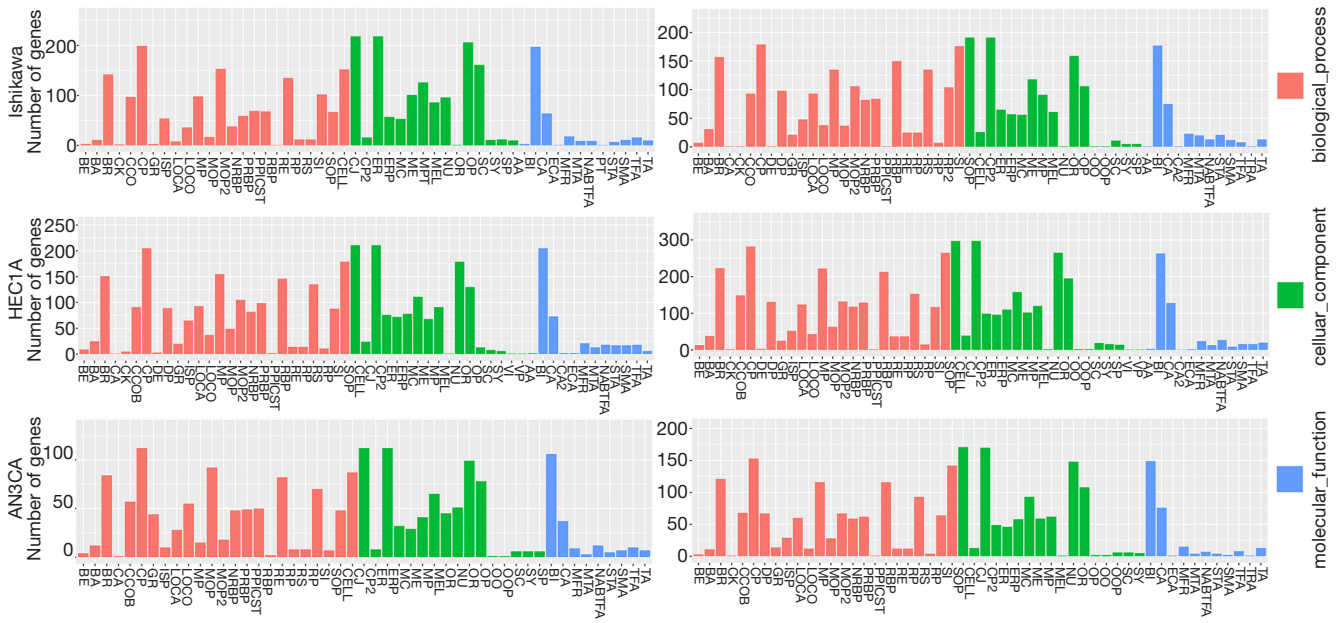

Figure 2 Annotation mapping enrichment analysis through GO database. Annotation mapping enrichment analysis of biological functions between H-CM and CM groups in Ishikawa, HEC1A and AN3CA cell line, by searching GO database entries (terms) for differential genes (q-value ≤0.05) and focused on the distribution of enriched gene sets represented by the abscissa at three GO terms: red bar for biological process, green bar for cellular component, blue bar for molecular function. The ordinate represents number of genes in different enrichment of biological functions. AA, antioxidant activity; BA, biological adhesion; BE, behavior; BI, binding; BR, biological regulation; CA, catalytic activity; CA2, chemorepellent activity; CCO, cellular component organization or biogenesis; CELL, cell; CJ, cell junction; CK, cell killing; CP, cell part; CP2, cellular process; DE, detoxification; ECA, electron carrier activity; ER, extracellular region; ERP, extracellular region part; GR, growth; ISP, immune system process; LOCA, localization; LOCO, locomotion; MC, macromolecular complex; ME, membrane; MEL, membrane-enclosed lumen; MFR, molecular function regulator; MOP, multi-organism process; MOP2, multicellular organismal process; MP, metabolic process; MPT, membrane part; MTA, molecular transducer activity; NABTFA, nucleic acid binding transcription factor activity; NRBP, negative regulation of biological process; NU, nucleoid; OR, organelle; OO, other organism; OOP, other organism part; OP, organelle part; RBP, regulation of biological process; RE, reproduction; PRBP, positive regulation of biological process; PT, protein tag; PPICST, presynaptic process involved in chemical synaptic transmission; RP, reproductive process; RP2, rhythmic process; RS, response to stimulus; SC, supramolecular complex; SI, signaling; SOP, single-organism process; SP, synapse part; SY, synapse; STA, signal transducer activity; SMA, structural molecule activity; TA, transporter activity; TFA, transcription factor activity, protein binding; VI, virion; VP, virion part.

Biological functions and signaling pathways response to hydrogen treatment in endometrial cancer cells

The coefficients of variation between H-CM and CM groups were determined through the enrichment P value (≤0.05) of genes and pathways using Fish's exact test. Mean expression levels were indicated by FPKM across samples, differentially expressed genes were identified through fold-change (FC) filtering. FC value of ≥1.0 indicates upregulated expression, while ≤–1.0 represents downregulated expression. FC value of ≥1.5 indicates significantly increased expression, while ≤–1.5 represents significantly reduced expression. Besides, FC of ≤–1.5 or ≥1.5 denotes a significantly activated or inhibited signaling pathway, respectively.

Among the 135 differentially expressed canonical pathways, 58 pathways were significantly downregulated and 77 pathways were significantly upregulated in the hydrogen-treated group compared to non-treated group (P≤0.05; *Table 1*). As we put emphasis on aspect of inflammatory and cell death in hydrogen treated endometrial cancer cells, GO pathway enrichment analysis demonstrated that the signaling pathways of TNF, NF-κB, apoptosis, necroptosis and ferroptosis (P≤0.05) were among the top 30 enriched pathways in hydrogen-treated HEC1A and AN3CA cells, and

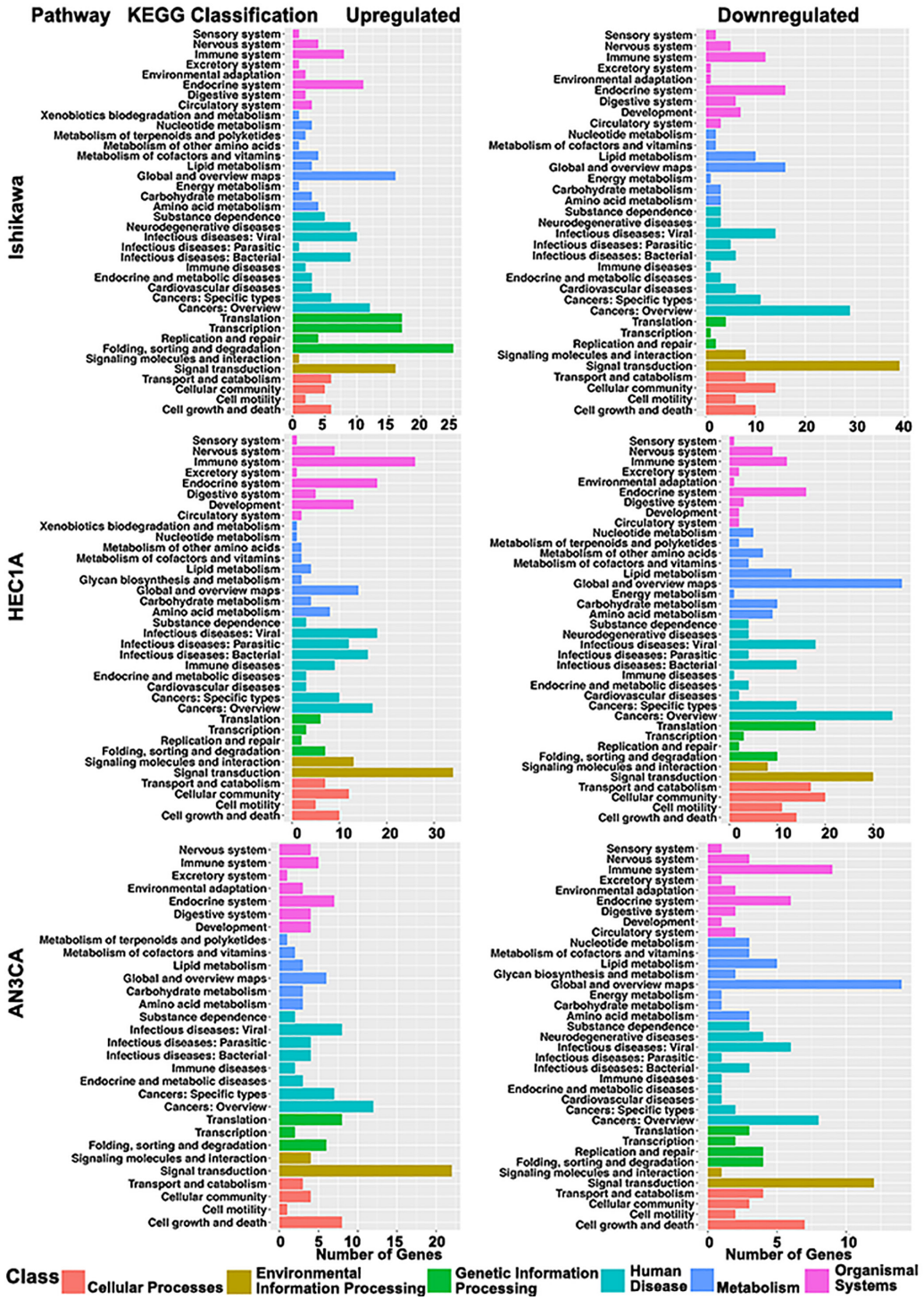

Figure 3 The coefficients of variation analyzed by KEGG database. The abscissa indicates coefficients of variation for the signaling pathways between H-CM and CM groups in Ishikawa, HEC1A and AN3CA cell line, or differential genes (q-value ≤0.05) analyzed by KEGG database. The ordinate indicates number of genes in different signaling pathways. Red bar represents cellular processes, brown bar represents environmental information processing, green bar represents genetic information processing, another green bar represents human disease, blue bar represents metabolism, purple bar represents organismal systems. KEGG, Kyoto Encyclopedia of Genes and Genomes; H-CM, hydrogen culture medium; CM, culture medium.

Table 1 Signaling pathways involved in hydrogen-treated endometrial cancer cells

Cell line	Up-regulated			Down-regulated		
	Gene		Significant pathway	Gene		Significant pathway
	log2(FC) =1–1.5	log2(FC) ≥1.5	P≤0.05	log2(FC) =–1 to –1.5	log2(FC) ≤–1.5	P≤0.05
Ishikawa	167	67	12	150	65	38
HEC1A	163	85	22	229	84	29
AN3CA	81	44	24	150	38	10
Total	411	196	58	529	187	77

FC, fold change.

TNF pathways ranged first in the GO pathway enrichment analysis in hydrogen-treated AN3CA cells (*Tables 2,3*, *Figure 4*), suggesting that the differential expressed genes are associated with inflammatory and cell death signaling pathways.

In addition, the results demonstrated a significant discordant regulation among the transcriptional levels of genes. Comparison between transcriptome and proteome data revealed that the expression patterns of proteins were correlated with their mRNA expression at transcription level. A total of 607 upregulated and 716 downregulated genes were identified in hydrogen-treated Ishikawa, HEC1A and AN3CA endometrial cancer cells compared to non-treated cells. The distributions of raw and filtered gene expression counts in TNF and NF-κB pathway are presented in *Tables 2,3* and *Figure 5A*. Notably, *JUN*, *JUNB*, *JUND*, *NFKBIA*, *NFKBID*, *NFKBIE*, *NFKBIZ*, *TNF*, *TNFAIP2*, *TNFAIP3* and *TNFRSF21* were upregulated in hydrogen-treated HEC1A cells, while *JUN*, *JUNB*, *NFKBIA* and *TNFFRSF12A* were upregulated in hydrogen-treated AN3CA cells [Log2 (FC) ≥1].

To highlight the importance of post-transcriptional processes, the protein levels of NF-κB, p-NFKBIA, NFKBIA and cleaved caspase-1 were detected by Western blotting. It was found that the levels of NF-κB, p-NFKBIA, NFKBIA and cleaved caspase-1 as well as p-NFKBIA/NF-κB ratio were significantly increased in H-CM group compared to CM group (P≤0.05; *Figure 5B*).

Hydrogen-induced apoptosis in endometrial cancer cells

Based on the above results, it was speculated that hydrogen could induce the apoptosis of endometrial cancer cells. The apoptotic rates of endometrial cancer cells were evaluated by FITC analysis using Annexin V-APC and PI staining. The percentage of apoptosis was calculated by the sum of up right (UR) and low right (LR) quadrant which represented the early phase of apoptosis. As shown in *Figure 6A*, Ishikawa and HEC1A cells exhibited significantly increased apoptotic rates after 24 h of hydrogen treatment compared to non-treated group (H-CM *vs.* CM; 4.60%±0.53% *vs.* 2.60%±0.16%, 6.53%±0.12% *vs.* 4.60%±0.06%, respectively; P≤0.05). To assess the possible role of hydrogen treatment in radiotherapy-induced apoptosis in endometrial cancer cells, the cultured Ishikawa and HEC1A cells were exposed to a ^{60}Co radiation source, in order to attain a desired dose of 7 Gy. Interestingly, there was significant difference in the apoptotic rate of radiotherapy-induced HEC1A cells between H-CM and CM groups (H-CM *vs.* CM; 5.10%±0.0026% *vs.* 3.07%±0.0082%, respectively; P=0.0079). Additionally, higher apoptotic rate of Ishikawa cells exposed to radiation was found in H-CM group compared to CM group (H-CM *vs.* CM; 4.83%±0.0086% *vs.* 2.83%±0.0047%), but not statistically significant (P=0.1115).

Overall, higher rates of apoptosis were observed in hydrogen-treated Ishikawa (H-CM *vs.* CM; 3.50%±0.1732% *vs.* 2.33%±0.0882%; P=0.0039) and AN3CA (H-CM *vs.* CM; 3.50%±0.1155% *vs.* 0.10%±0.0577%; P<0.0001) cells. Intriguingly, pre-incubated with 5 mM of ROS generation blocker N-acetylcysteine (NAC) 1 h before treatment with hydrogen inversely decreased the apoptotic rates of hydrogen-treated Ishikawa (H-CM *vs.* H-CM+NAC; 4.83%±0.0086% *vs.* 2.1%±0.1155%; P=0.0025) and AN3CA (H-CM *vs.* H-CM+NAC; 3.50%±0.1155% *vs.* 2.1%±0.0577%; P=0.0004) cells (*Figure 6B*).

Similar results were obtained for hydrogen-treated HEC1A (P=0.000613) cells, as demonstrated by Annexin V-APC/PI double staining method (*Figure 7A*). To further characterize the markers of hydrogen-induced apoptosis in endometrial cancer cells, Western blotting was used

to examine the levels of caspase-3, cleaved caspase-3 and cleaved caspase-9. Notably, the expression levels of these apoptotic proteins were significantly increased in hydrogen treated HEC1A cells (*Figure 7B*).

Discussion

Necroptosis, ferroptosis and apoptosis are distinct cell death processes that cooperate in the presentation and clearance of invading pathogens (16). Necroptotic and ferroptotic cell deaths are induced by the ligands of TNF receptor superfamily and toll-like receptor (TLR) (17), while apoptosis is triggered by cytokine TNF-α-mediated intrinsic pathway after interacted with specific membrane receptors and Caspase-3/-7/-8/-9 (17). The secretion of TNF-α is regulated by NF-κB activation (18). At both early and late times of infection, cell death is correlated with an increased TNF-α production, which subsequently bind to its receptor, such as TNFR, leading to an activation of caspase-8, and thereby triggering cell apoptosis pathway.

In resting cells, NF-κB complex is maintained in the cytoplasm as a dimer consisting of NF-κB, NF-κB1 (p50), Rel-A (p65) and NF-κB2 (p52) subunits. After being bound to inhibitory IκB protein family (e.g., IκBα, IκBβ, IκBγ, IκBδ, IκBε, IκBζ, IκB-R, Bcl-3, p100 and p105), IkappaB kinase complex (IKK) is formed, keeping NF-κB pool mainly in the cytoplasm by inhibiting its nuclear localization, accumulation, transactivation and association with DNA (19,20). IκBα, encoded by NF-κB inhibitor-alpha (*NFKBIA*), is the most abundant and critical inhibitor of NF-κB (21). The priming phase of apoptosis is triggered by the first signals, including lipopolysaccharides (LPS) and damage-associated molecular patterns (DAMP). IκBα is

Table 2 The significant affected pathways in hydrogen-treated endometrial cancer cells

Pathway	P value	
	HEC1A	AN3CA
TNF	4.35E−09	0.001093492
NF-κB	2.90E−05	0.021789819
Apoptosis	0.032489587	0.003746339
Necroptosis	0.021919497	–
Ferroptosis	–	0.01172137

Genes in the signaling pathways of TNF, NF-κB, apoptosis, necroptosis and ferroptosis were significantly upregulated. Both TNF and NF-κB signaling pathways in HEC1A and AN3CA cells were regulated by hydrogen treatment.

Table 3 The significant affected genes in hydrogen-treated endometrial cancer cells

Gene	HEC1A			AN3CA		
	H-CM	CM	Log2(FC)	H-CM	CM	Log2(FC)
NFKBIA	103.5338	20.9748	2.3034	11.5170	4.2156	1.4500
NFKBID	13.9361	1.1728	3.5708	–	–	–
NFKBIE	16.0616	5.5589	1.5307	–	–	–
NFKBIZ	19.8233	5.2468	1.9177	–	–	–
TNF	83.2268	4.4283	4.2322	–	–	–
TNFFRSF12A	–	–	–	72.5851	32.6434	1.1529
TNFAIP2	89.2708	30.6025	1.5445	–	–	–
TNFAIP3	8.7570	1.1613	2.9147	–	–	–
TNFRSF21	17.6954	7.5398	1.2308	–	–	–
JUN	75.7223	12.9895	2.5434	22.3262	7.0776	1.4264
JUNB	210.8038	64.9215	1.6991	69.6526	31.2481	1.1564
JUND	24.9834	12.4495	1.0049	–	–	–

Genes in the signaling pathways of TNF, NF-κB, apoptosis, necroptosis and ferroptosis were significantly upregulated. Both TNF and NF-κB signaling pathways in HEC1A and AN3CA cells were regulated by hydrogen treatment. H-CM, hydrogen culture medium; CM, culture medium; FC, fold change.

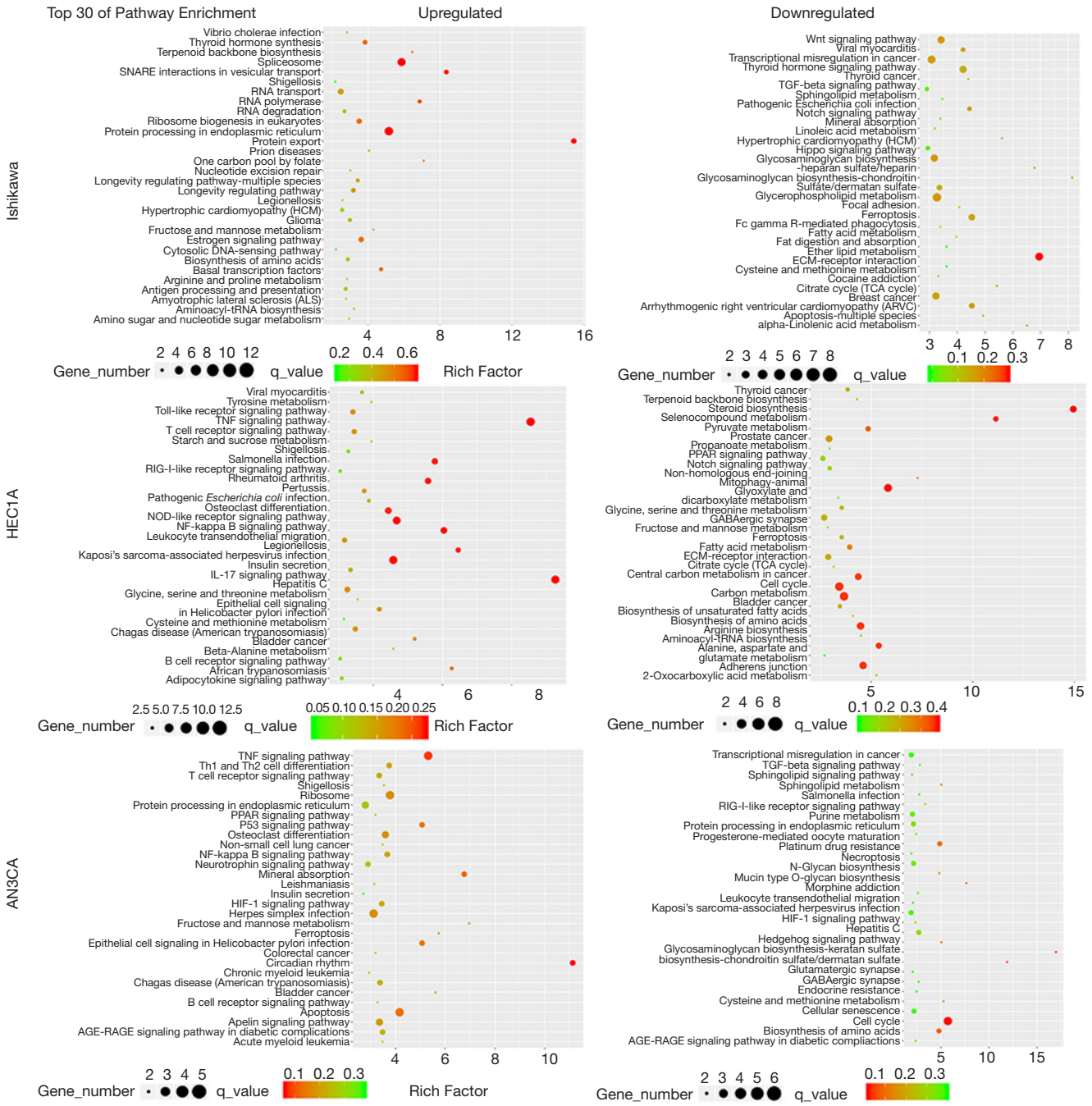

Figure 4 Top 30 enriched pathways of hydrogen-treated endometrial cancer cells. The top 30 pathways enriched by rich factor in the abscissa between H-CM and CM groups in Ishikawa, HEC1A and AN3CA cell line. The color of the point indicates the significance level (q-value) of GO. The shape point indicates major categories of GO database the corresponding GO entry belongs to the size of the point represented the number of genes mapped into the GO entry. GO, Gene Ontology; H-CM, hydrogen culture medium; CM, culture medium.

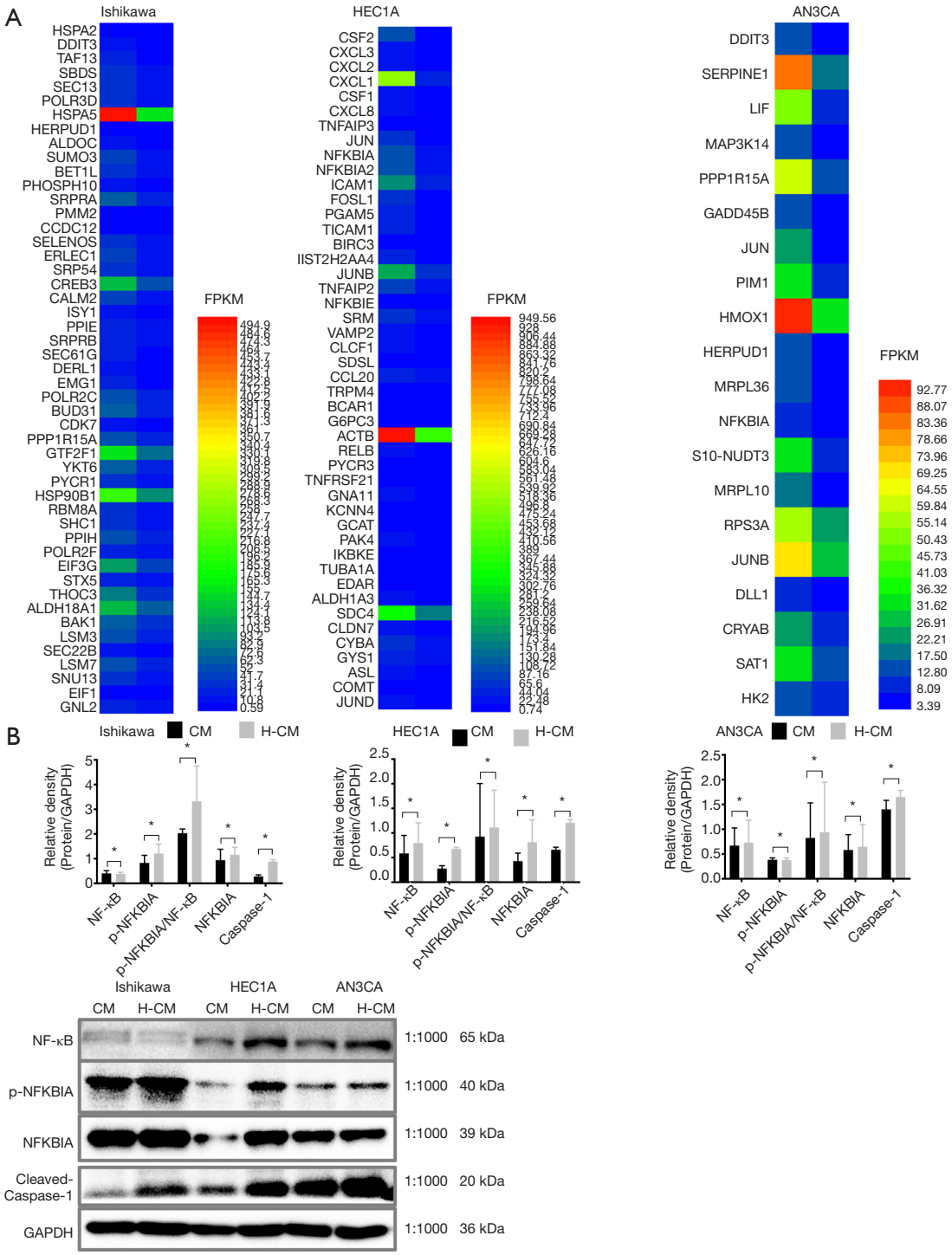

Figure 5 Expression patterns of genes involved in TNF and NF-κB signaling pathways. (A) Heat map of the genes involved in TNF, NF-κB, apoptosis, necroptosis and ferroptosis signaling pathways between H-CM and CM groups in Ishikawa, HEC1A and AN3CA cell line (P≤0.05). Each small box represents a gene, and its FPKM values is indicated by different colors. (B) NF-κB, p-NFKBIA, NFKBIA, p-NFKBIA/NF-κB and cleaved caspase-1 were significantly increased in hydrogen-treated Ishikawa, HEC1A and AN3CA cells compared to non-treated group, as determined by Western blot analysis. GAPDH was used as a loading control. Data are presented as mean ± SD. *, P≤0.05. H-CM, hydrogen culture medium; CM, culture medium; SD, standard deviation.

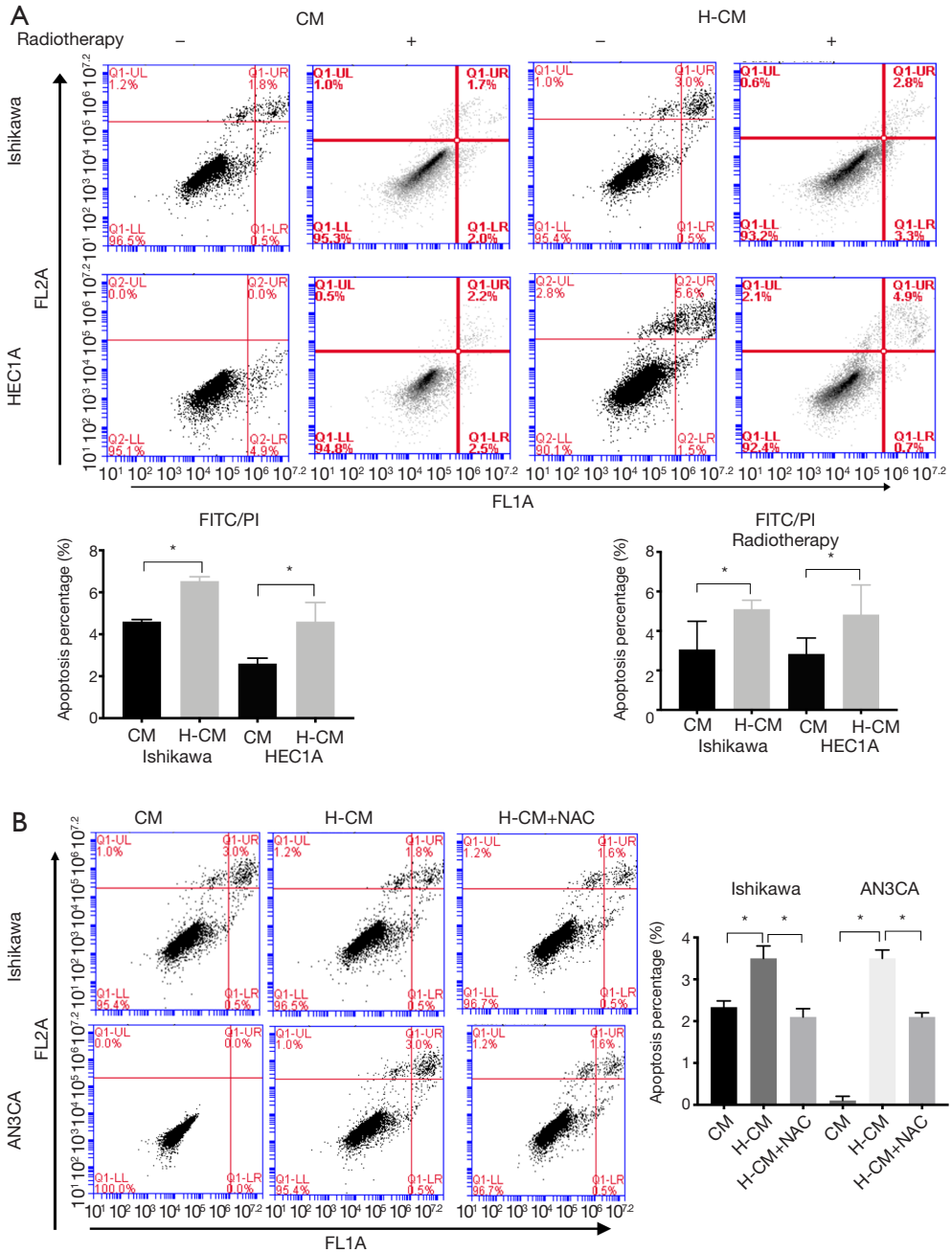

Figure 6 Apoptotic rates of hydrogen-treated endometrial cancer cells. (A) The percentages of apoptosis were significantly increased in hydrogen-treated Ishikawa (H-CM *vs.* CM; 4.60%±0.53% *vs.* 2.60%±0.16%; P=0.0221) and HEC1A (H-CM *vs.* CM; 6.53%±0.12% *vs.* 4.60%±0.06%; P<0.0001) cells compared to non-treated cells. Three hours after radiation of a 60Co source, at a dose of 7 Gy, the apoptotic rates of the three endometrial cancer cells were evaluated by FITC Annexin V apoptosis method. Hydrogen-treated Ishikawa (H-CM *vs.* CM; 4.83%±0.0086% *vs.* 2.83%±0.0047%; P=0.1115) and HEC1A (H-CM *vs.* CM 5.10%±0.0026% *vs.* 3.07%±0.0082%; P=0.0079) cells exhibited higher apoptotic rates compared to CM-treated cells. (B) Increased percentages of apoptotic cells were found in hydrogen-treated Ishikawa (H-CM *vs.* CM; 3.50%±0.1732% *vs.* 2.33%±0.0882%; P=0.0039) and AN3CA (H-CM *vs.* CM; 3.50%±0.1155% *vs.* 0.10%±0.0577%; P≤0.0001) cells. ROS generation blocker NAC (5 mM) inversely decreased the apoptotic rates of hydrogen-treated Ishikawa (H-CM *vs.* H-CM+NAC 4.83%±0.0086% *vs.* 2.1%±0.1155%; P=0.0025) and AN3CA (H-CM *vs.* H-CM+NAC 3.50%±0.1155% *vs.* 2.1%±0.0577%; P=0.0004) cells. Data are presented as mean ± SD. *, P≤0.05 compared with non-treated group. H-CM, hydrogen culture medium; CM, culture medium; NAC, N-acetylcysteine; FITC, fluorescein isothiocyanate.

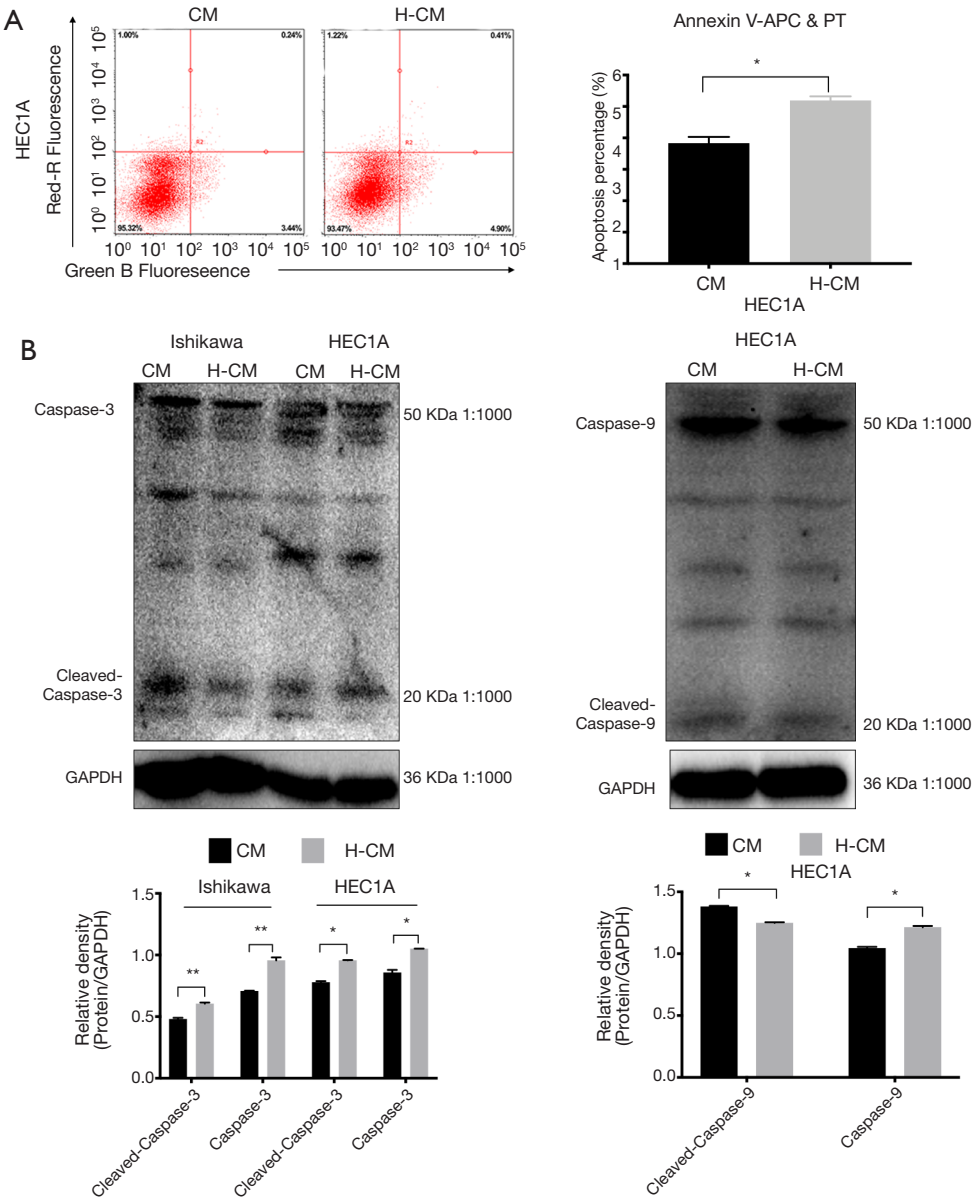

Figure 7 Apoptosis markers for hydrogen-treated endometrial cancer cells. (A) The apoptotic rates of hydrogen-treated HEC-1A (H-CM *vs.* CM; 5.19%±0.1355% *vs.* 3.83%±0.1999%; P=0.000613) cells were significantly increased compared to non-treated cells, as demonstrated by Annexin V-APC/PT method. (B) The levels of caspase-3, cleaved caspase-3 and cleaved caspase-9 in HEC1A cells with 24 h of hydrogen treatment were significantly higher than those in non-treated group, as revealed by relative optical density image analysis. Data are presented as mean ± SD. *, P≤0.05 compared with non-treated group. APC, allophycocyanin; FITC, fluorescein isothiocyanate; H-CM, hydrogen culture medium; CM, culture medium.

ubiquitinated and degraded, resulting in NF-κB activation through phosphorylation of TLRs in the stimulated cells, which rapidly localized to the nucleus to allow the transcription of proinflammatory cytokines, such as TNF-α, IL-1β and IL-6 (5,22,23), thus ultimately contributing to tumor cell apoptosis. The second delayed priming phase activates several signaling pathways, such as TNF-α that suppresses phosphor-NF-κB/p65 expression, and further induces a wide spectrum of inflammatory reactions by producing adenosine triphosphate (ATP), and eventually

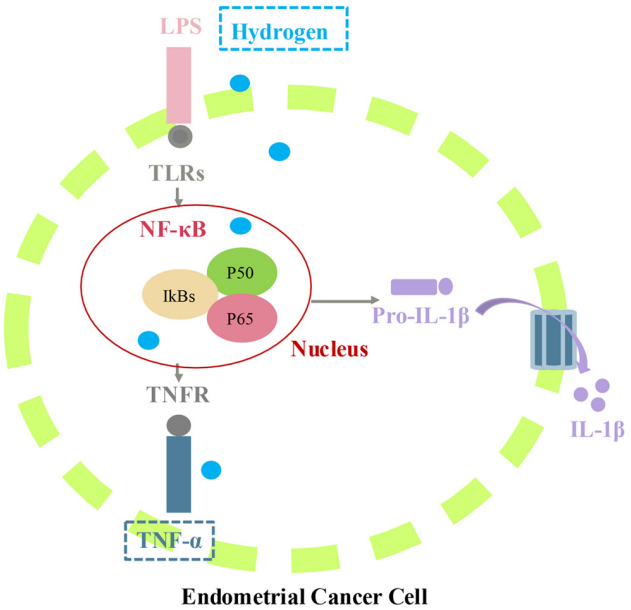

Figure 8 A proposed model depicting the potential mechanisms of hydrogen-mediated cell apoptosis via a positive feedback regulation of TNF/NF-κB inflammasome pathway. TLRs induces the activation of NF-κB pathway, and promotes the expression levels of inflammatory genes such as TNF-α and IL-1β. Hydrogen penetrates across biomembranes and diffuses into the cytosol, mitochondria and nucleus, leading to the increased expression levels of TNF-α, NF-κB and IL-1β, and eventually triggers cell apoptosis. TLR, toll-like receptor; LPS, lipopolysaccharides; TNFR, tumor necrosis factor receptor.

lead to cell injury caused by the release of proinflammatory cytokines (24,25).

Obesity and insulin resistance have been considered as risk factors for endometrial cancer. Additionally, TNF-α, IL-1β, NF-κB have been shown to induce endometrial cancer cell apoptosis in a dose- and time-dependent manner. Studies on excised human tissue demonstrate that NF-κB family members are highly expressed in proliferative endometrium, endometrial hyperplasia and endometrial carcinoma (26,27). Besides, TNF-α-induced apoptosis are observed in Ishikawa and AN3CA endometrial cancer cell lines. These proinflammatory cells can then feed back into NF-κB pathway, further enhancing the proinflammatory and apoptotic processes (28,29).

Considering that hydrogen can easily dissipate across cells throughout the body, hydrogen water or hydrogen-rich saline is increasingly accepted as a promising therapeutic approach, due to lack of adverse effects (8). Hydrogen might exert a biphasic effect of activating inflammatory pathway in tumor cell and inhibiting inflammatory pathway in normal cells. Hydrogen can be applied to treat inflammatory diseases, as hydrogen treatment reduces the expression levels of pro-inflammatory factors such as TNF-α, IL-6 and IL-1β in non-cancerous cells (30,31). Hydrogen water not only inhibits the clonal growth of human tongue carcinoma cells, but also suppresses the invasion of human fibrosarcoma cells concurrently with intracellular oxidant repression, as well as scavenged intracellular oxidants (e.g., hydrogen peroxides) (32). Inhalation of 1% hydrogen gas or drinking hydrogen water can alleviate the nephrotoxicity, mortality and body-weight loss caused by cisplatin, and does not compromise the anti-tumor effects of cisplatin against cancer cell lines *in vitro* and tumor-bearing mice *in vivo* (9,33). Nevertheless, whether hydrogen can be used to treat endometrial cancer has not yet been reported.

Our results demonstrated that hydrogen treatment activated TNF/NF-κB, apoptosis, necroptosis and ferroptosis signaling pathways in endometrial cancer cells ($P \leq 0.05$), as revealed by RNA sequencing analysis. In addition to the GO analysis, KEGG pathway enrichment analysis was used to further elucidate the functional mechanisms underlying hydrogen treatment. Correlation analysis between transcriptome and proteome demonstrated that the enrichment of proteins in different GO terms was consistent with the transcriptomic results. However, the enriched pathways at protein level were specifically grouped as genetic information processing, while various metabolic processes were dominated at transcriptomic level. The molecular pathways underlying cancer inflammation involve NF-κB transcription factor and its inhibitory IKK complex. In this study, NFKBIA, NFKBID, NFKBIE, NFKBIZ, TNF, TNFAIP2, TNFAIP3, TNFRSF21, TNFFRSF12A, JUN, JUNB, JUND were found to be upregulated in hydrogen-treated endometrial cancer cells. These results, taken together, suggest that these upregulated genes play pivotal roles in hydrogen-induced apoptosis in endometrial cancer (*Figure 8*). To further explore the effects of post-transcriptional regulation on hydrogen-induced apoptosis, the proteins that went against the overall trend of concordant gene regulation were investigated at protein level.

However, there was limitations in our study since the research was only an RNA sequencing analysis of signaling pathways and functional gene groups in hydrogen-treated endometrial cancer cells. How hydrogen induces TNF/NF-κB and thereafter causes apoptosis pathways in endometrial cancer cells should be explained on further research. Taken

altogether, our data indicate that hydrogen treatment can induce endometrial cancer cell apoptosis via TNF/NF-κB pathway activated by proinflammatory cytokines. Therefore, hydrogen may be a promising therapeutic target for endometrial cancer.

Acknowledgments

We thank Shanghai Yiquan Investment Limited Partnership Company provided hydrogen water. We thank LetPub (www.letpub.com) for its linguistic assistance during the preparation of this manuscript.
Funding: This study was supported by National Natural Science Foundation of China (No. 81902628) and Translational Medicine Cross Research Fund of Shanghai Jiao Tong University School of Medicine (No. ZH2018QNB08).

Footnote

Conflicts of Interest: All authors have completed the ICMJE uniform disclosure form (available at http://dx.doi.org/10.21037/tcr.2020.03.71). The authors have no conflicts of interest to declare.

Ethical Statement: The authors are accountable for all aspects of the work in ensuring that questions related to the accuracy or integrity of any part of the work are appropriately investigated and resolved.

References

1. Siegel RL, Miller KD, Jemal A. Cancer statistics, 2019. CA Cancer J Clin 2019;69:7-34.
2. Fathy SA, Mohamed MR, Ali MAM, et al. Influence of IL-6, IL-10, IFN-γ and TNF-α genetic variants on susceptibility to diabetic kidney disease in type 2 diabetes mellitus patients. Biomarkers 2019;24:43-55.
3. Lin CC, Edelson BT. New Insights into the Role of IL-1β in Experimental Autoimmune Encephalomyelitis and Multiple Sclerosis. J Immunol 2017;198:4553-60.
4. Coussens LM, Werb Z. Inflammation and cancer. Nature 2002;420:860-7.
5. Yan Y, Jiang W, Liu L, et al. Dopamine Controls Systemic Inflammation through Inhibition of NLRP3 Inflammasome. Cell 2015;160:62-73.
6. Kamimura N, Nishimaki K, Ohsawa I, et al. Molecular Hydrogen Improves Obesity and Diabetes by Inducing Hepatic FGF21 and Stimulating Energy Metabolism in db/db Mice. Obesity 2011;19:1396-403.
7. Zhao L, Wang Y, Zhang G, et al. L-Arabinose Elicits Gut-Derived Hydrogen Production and Ameliorates Metabolic Syndrome in C57BL/6J Mice on High-Fat-Diet. Nutrients 2019. doi: 10.3390/nu11123054.
8. Chen H, Zhou C, Xie K, et al. Hydrogen-rich Saline Alleviated the Hyperpathia and Microglia Activation via Autophagy Mediated Inflammasome Inactivation in Neuropathic Pain Rats. Neuroscience 2019;421:17-30.
9. Nakashimakamimura N, Mori T, Ohsawa I, et al. Molecular hydrogen alleviates nephrotoxicity induced by an anti-cancer drug cisplatin without compromising anti-tumor activity in mice. Cancer Chemother Pharmacol 2009;64:753-61.
10. Zhong Z, Zhai Y, Liang S, et al. TRPM2 links oxidative stress to NLRP3 inflammasome activation. Nat Commun 2013;4:1611-21.
11. Ohsawa I, Ishikawa M, Takahashi K, et al. Hydrogen acts as a therapeutic antioxidant by selectively reducing cytotoxic oxygen radicals. Nat Med 2007;13:688-94.
12. Uto K, Que W, Sakamoto S, et al. Hydrogen Rich Solution Attenuates Cold Ischemia-Reperfusion Injury in Rat Liver Transplantation. BMC Gastroenterol 2019;19:25-33.
13. Li L, Liu T, Liu L, et al. Effect of hydrogen-rich water on the Nrf2/ARE signaling pathway in rats with myocardial ischemia-reperfusion injury. J Bioenerg Biomembr 2019;51:393-402.
14. Zhang J, Zhou H, Liu J, et al. Protective effects of hydrogen inhalation during the warm ischemia phase against lung ischemia-reperfusion injury in rat donors after cardiac death. Microvasc Res 2019;125:103885.
15. Eryilmaz S, Turkyilmaz Z, Karabulut R, et al. The effects of hydrogen-rich saline solution on intestinal anastomosis performed after intestinal ischemia reperfusion injury. J Pediatr Surg 2019. [Epub ahead of print].
16. Jorgensen I, Rayamajhi M, Miao EA. Programmed cell death as a defence against infection. Nat Rev Immunol

2017;17:151-64.
17. Fuentes-Prior P, Salvesen GS. The protein structures that shape caspase activity, specificity, activation and inhibition. Biochem J 2004;384:201-32.
18. Ooppachai C, Limtrakul DP, Yodkeeree S. Dicentrine Potentiates TNF-alpha-Induced Apoptosis and Suppresses Invasion of A549 Lung Adenocarcinoma Cells via Modulation of NF-kappaB and AP-1 Activation. Molecules 2019. doi: 10.3390/molecules24224100.
19. Zhang G, Li J, Purkayastha S, et al. Hypothalamic programming of systemic ageing involving IKK-β, NF-κB and GnRH. Nature 2013;497:211-6.
20. Zhang Q, Lenardo MJ, Baltimore D. 30 Years of NF-κB: A Blossoming of Relevance to Human Pathobiology. Cell 2017;168:37-57.
21. Coto E, Reguero JR, Avanzas P, et al. Gene variants in the NF-KB pathway (NFKB1, NFKBIA, NFKBIZ) and risk for early-onset coronary artery disease. Immunol Lett 2019;208:39-43.
22. Maninjay KA, Jonathan AH. Uncoupling of Pyrin-only protein 2 (POP2)-mediated dual regulation of NF-κB and the inflammasome. J Biol Chem 2011;286:40536-47.
23. Staples E, Morillo-Gutierrez B, Davies J, et al. DisseminatedMycobacterium malmoenseandSalmonellaInf ections Associated with a Novel Variant inNFKBIA. J Clin Immunol 2017;37:415-8.
24. Bauernfeind F, Niepmann S, Knolle PA, et al. Aging-Associated TNF Production Primes Inflammasome Activation and NLRP3-Related Metabolic Disturbances. J Immunol 2016;197:2900-8.
25. Yu-Rice Y, Edassery SL, Urban N, et al. Selenium-Binding Protein 1 (SBP1) autoantibodies in ovarian disorders and ovarian cancer. Reproduction 2017;153:277-84.
26. Pallares J, Martínezguitarte JL, Dolcet X, et al. Abnormalities in the NF-kappaB family and related proteins in endometrial carcinoma. J Pathol 2004;204:569-77.
27. Vaskivuo TE, Stenbäck F, Tapanainen JS. Apoptosis and apoptosis-related factors Bcl-2, Bax, tumor necrosis factor-alpha, and NF-kappaB in human endometrial hyperplasia and carcinoma. Cancer 2002;95:1463-71.
28. Pikarsky E, Porat RM, Stein I, et al. NF-kappaB functions as a tumour promoter in inflammation-associated cancer. Nature 2004;431:461-6.
29. Karin M, Benneriah Y. Phosphorylation Meets Ubiquitination: The Control of NF-κB Activity. Annu Rev Immunol 2000;18:621-63.
30. Hattori Y, Kotani T, Tsuda H, et al. Maternal molecular hydrogen treatment attenuates lipopolysaccharide-induced rat fetal lung injury. Free Radic Res 2015;49:1026-37.
31. Li J, Wu X, Chen Y, et al. The Effects of Molecular Hydrogen and Suberoylanilide Hydroxamic Acid on Paraquat-Induced Production of Reactive Oxygen Species and TNF-α in Macrophages. Inflammation 2016;39:1990-6.
32. Saitoh Y, Okayasu H, Xiao L, et al. Neutral pH hydrogen-enriched electrolyzed water achieves tumor-preferential clonal growth inhibition over normal cells and tumor invasion inhibition concurrently with intracellular oxidant repression. Oncol Res 2008;17:247-55.
33. Fransson AE, Marta K, Kristian P, et al. Hydrogen Inhalation Protects against Ototoxicity Induced by Intravenous Cisplatin in the Guinea Pig. Front Cell Neurosci 2017;11:280-92.

Cite this article as: Yang Y, Liu YP, Bao W, Chen JS, Xi XW. RNA sequencing analysis reveals apoptosis induction by hydrogen treatment in endometrial cancer via TNF and NF-κB pathways. Transl Cancer Res 2020;9(5):3468-3482. doi: 10.21037/tcr.2020.03.71

